

ТЕОРИЯ И ТЕХНИКА УСКОРЕНИЯ ЧАСТИЦ

ON A METHOD OF TUNING OF COUPLERS FOR ELECTRON LINACS BASED ON DISK LOADED WAVEGUIDES

*N.I. Aizatskiy, K.Yu. Kramarenko, I.V. Khodak, V.A. Kushnir, V.V. Mytrochenko,
A.M. Opanasenko, S.A. Perezhogin, L.I. Selivanov, V.F. Zhiglo
National Science Center "Kharkov Institute of Physics and Technology", Kharkov, Ukraine
E-mail: mitvic@kipt.kharkov.ua*

The article presents an adjustment procedure for an input and output couplers of a traveling wave accelerating section based on cylindrical disk loaded waveguide (CDLW). The procedure consists in bead pull measurement of on axis field and calculation of reflection from the coupler under adjustment using the field values at three points separated by a geometric period of the adjacent CDLW. Description of a model for coupler tuning as well as tuning results also are presented.

PACS: 29.20.Ej

INTRODUCTION

An accelerating section for the industrial electron linac that is under development at NSC KIPT is based on the CDLW [1]. The section contains a buncher with smoothly varying phase velocity to ensure efficient capture of low energy beam during the initial acceleration. Couplers are used for input of high frequency (rf) power to the structure (input coupler) and for removing of its unused part (output coupler). Usually, for reaching low reflections from section, the couplers must be tuned experimentally. The traditional technique of coupler tuning is based on the analysis of reflection coefficient change in a waveguide connecting the generator of rf-power with the coupler when the reflecting plunger or the absorber is moved along structure with a step of DLW period. It is assumed that inaccuracies in section manufacturing are absent (see, for example, [2]). The main problem of such method is manufacturing of sufficiently long part of the section (not less than six periods) without the inaccuracies. For inhomogeneous accelerating section with variable phase velocity this is probably impossible because the exact cell sizes are generally unknown.

Design feature of the developed section is that the first two and the last two cells are the same in pairs. Therefore our goal is to obtain such coupler tuning technique in which part of the section without the inaccuracies of manufacturing would be minimal.

1. COUPLER TUNING TECHNIQUE

In [3, 4] the tuning technique based on measuring of the fields in three adjacent cells by the method of non-resonant perturbation is used. Method of finding the reflection from the coupler using the field values at three points separated by a distance that is equal to the geometric period of the structure is proposed in [5]. Criterion of applicability of the technique for the regions where the periodicity is violated (the coupler regions) is also obtained in this paper.

Assume that the complex field amplitude in the travelling wave section $E_c(z)$ can be represented as superposition of forward and backward waves with the real positive phase function $\phi(z)$. Introducing a complex reflection coefficient R from inhomogeneity (from coupler), we can represent the electric field as:

$$E_c(z) = E(z) \left[e^{-j\phi(z)} + R e^{j\phi(z)} \right]. \quad (1)$$

From Floquet's theorem it follows that fields through the structure period D differs only by a phase factor, which corresponds to a phase shift ψ per period. In this case [5]

$$\cos(\psi) = \frac{E_c(z-D) + E_c(z+D)}{2E_c(z)}, \quad (2)$$

$$R \cdot e^{2j\phi} = \frac{2\sin(\psi) - j \frac{E_c(z-D) - E_c(z+D)}{2E_c(z)}}{2\sin(\psi) + j \frac{E_c(z-D) - E_c(z+D)}{2E_c(z)}}, \quad (3)$$

where $E_c^2(z) e^{2j\phi} = E^2(z) [1 + R \cdot e^{2j\phi}]^2$,

$$E^2(z) = |E_c(z)|^2 / [1 + |R|^2 + 2 \cdot \text{real}(R \cdot e^{2j\phi})].$$

In homogeneous CDLW (far from inhomogeneities) the Floquet theorem conditions are fulfilled, waves propagate without reflections, so $|R|$ and $\cos(\psi)$ in Eqs. (2, 3) do not depend on the longitudinal coordinate z . Near the coupler these values are functions of z [5], because to satisfy the boundary conditions in the coupler electromagnetic field must contains evanescent waves. When moving away from the coupler, evanescent waves attenuate. The question is at what distance from the coupler these components can be neglected in order to use the considered tuning technique. In [6] the model consisting of 4 cells and two couplers was used for simulation. At a distance of about two periods from the coupler the evanescent waves influence on the field distribution insignificantly. Based on this we propose the following model for coupler tuning (Fig. 1). The model is composed of coupler, two first cells of the accelerating section for an input coupler (or two last cells for output coupler) and one additional cell with an additional coupler (shadowed part in Fig. 1).

Thus for tuning model we need to have 4 identical discs and 3 rings. Each ring attached to corresponding disc is tuned using technique [7] taking into account the correction on vacuum, brazing fillets and difference of ambient temperature from section operating temperature. In order to tune mostly the size of the coupling hole, the preliminary tuning of cell radius is necessary. It should be noted that in our design the coupling hole is

shaped as a rectangular window. The length of the hole coincides with the length of the coupler cell and is the constant value at the tuning, so only the width of the hole is the subject for change. Since the coupler construction does not allow a change of frequency within the wide limits ($\leq \pm 2$ MHz), the radius of coupler ring has to provide the frequency within that range. We take the radius value basing on our previous experience in coupler fabrication. The coupler radius can be also obtained with a 3D electromagnetic code.

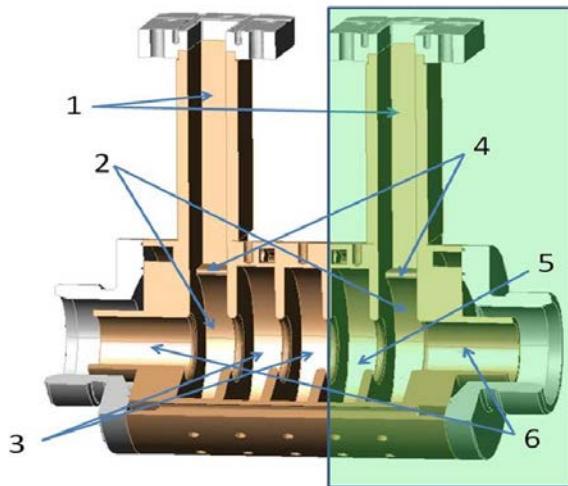


Fig. 1. Model for coupler tuning. 1 are rectangular waveguides; 2 are coupler cells; 3 are regular cells of the section; 4 are coupling holes; 5 is additional cell; 6 are evanescent parts of coupler cells

At fabrication of the model cells it is much simpler to measure the cavity frequency than the cavity diameter. Therefore each step of tuning can be simulated using the SUPERFISH code [8]. In particular the SUPERFISH model shown in Fig. 2 was used to determine the eigenfrequency of coupler cell.

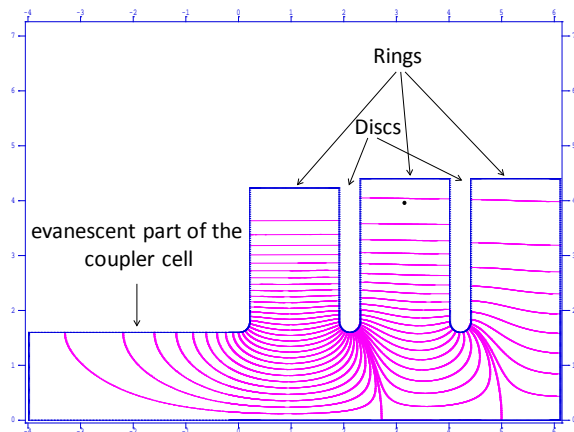


Fig. 2. SUPERFISH model for obtaining of eigenfrequency of coupler cell

This model consists of the coupler cell with the fragment of evanescent waveguide for beam input and two adjacent cavities of the section. Radii of the section cavities used in simulation were obtained from the equation $b = c\nu_{010}/f$, where f is the measured frequency of E_{010} mode of a pillbox cavities formed by the rings and flat walls, c is the velocity of light, ν_{010} is the Bessel function root.

Simulation model has three eigenfrequencies. At the highest frequency the maximum of the field is in the coupler (see Fig. 2). Therefore the value of this frequency is the most sensitive to the value of the coupler radius.

At preliminary tuning of the coupler cell the frequency of the model was adjusted to the calculated one by diamond turning of the coupler ring taking into account the mention above correction.

It should be noted that the layout shown in Fig. 2 needs two regular cells, and for the layout in Fig. 1 it is necessary to adopt three of such cells, so the middle cell was used in both cases.

Parameters of the model for coupler tuning are presented in Table 1.

Table 1
Parameters of the model for coupler tuning

Parameters	Input coupler	Output coupler
Operating frequency, MHz	2856	2856
Period, mm	20.792	34.99
Disc thickness, mm	4	4
Length of ring in regular cell, mm	16.792	30.99
Length of ring in coupler, mm	16,792	34
Radius of aperture, mm	16	12.056
Radius of ring in regular cell, mm	44.000	41.335
Radius of ring in coupler, mm	42.308	40.4
Number of periods of regular part	3	3

After the coupler cell frequencies had been preset to the calculated ones both parts of the model shown in Fig. 1 (without rectangular waveguides and coupling holes) were brazed separately. To measure eigenfrequencies the model was excited by antennas located in an evanescent portion of the coupler. For input coupler measured eigenfrequencies gave satisfactory agreement with simulated ones (Table 2). Another picture was observed for output coupler. The resonant frequency of the coupler cell is far outside the bandwidth of the travelling wave section with $a = 12.056$ mm. Therefore the coupling between couplers was so week that resonant curve had only one peak.

Table 2
Eigenfrequencies of the model for input coupler

RF test frequency, MHz	Simulated frequency, MHz	Difference, MHz
2944.068	2945.58	1.5120
2940.296	2941.92	1.6240
2857.78	2857.46	-0.3200
2783.578	2784.39	0.8120
2719.464	2719.94	0.4760

After brazing of the two parts of the model (see Fig. 1) notches for rectangular waveguides were fabricated. The notch in the input coupler was performed by electrospark cutting and in the output coupler it was performed by milling. The segment of rectangular waveguide with flange was fitted to the

notch of input coupler. The fitting accuracy ensured the capillary wetting of the surfaces in subsequent brazing. Short segments of the stainless steel waveguides were brazed into notches of the output couplers. Rectangular copper waveguide with flange have to be welded to the segment after joining of the output coupler to the accelerating section.

To adjust the size of coupling hole, it is necessary to disconnect the rectangular waveguide from the coupler, and that waveguide should be firmly pressed to ensure electrical contact when reflection coefficient is measured. Quick connection and disconnection of waveguides were provided with the system of cable wires and handles that operated as a catch clip. Two parts of the model were pressed together by using three rods (Fig. 3). The model was set to the platform, where the bead pull mechanism was located. Unambiguity of setting of the model over the longitudinal coordinate was provided by its connection with the input rectangular waveguide. The position of rectangular waveguide does not change. Unambiguity of setting of the model over the transversal coordinates was provided by cylindrical supports under flanges, which ensure the contraction of two parts of the model. Output coupler was tuned in analogous stand. The difference was that the waveguides was pressed to the short segments of the stainless steel waveguides.

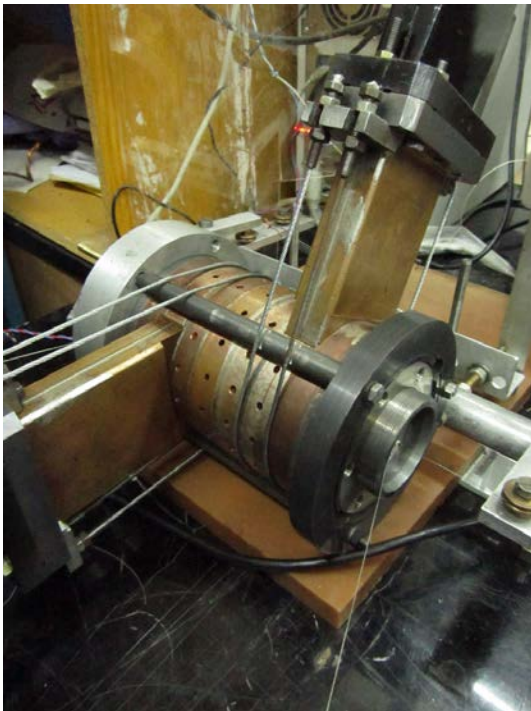


Fig. 3. Stand for input coupler adjustment

At coupler adjustments one of the couplers was connected through the measuring directional coupler to the network analyzer HP 8753, and the second one to a matched load. The process of the bead pull measurement was performing using a personal computer running specially developed software.

2. TUNING RESULTS

Initial size of the coupling hole in the input coupler was 30 mm. The measured value of the element S_{11} of a scattering matrix was 0.9 in this case (Fig. 4). It should be noted that R (see Eq.(3)) was measured with

considerable error at such value of S_{11} because it was necessary to distinguish the contribution of the reflection from the bead on the background of a significant reflection from the coupler. In this regard, we averaged both the raw data (HP 8753 was operated at the averaging factor of 8 or even 16) and the R coefficient data calculated at several measurement sessions. In order to decide what we need to adjust (hole size or cell frequency) several experiments were conducted. It was found that the main reaction of R on changes in the coupler is the following: imaginary part of R reacts on the cell frequency. The higher the frequency, the smaller the imaginary part of R . Based on the obtained data coupling holes of the both couplers were widened simultaneously to the value of 34.5 mm and then each hole was widened alternately. Dependence of the global coefficient S_{11} on the size of coupling hole L is shown in Fig. 4.

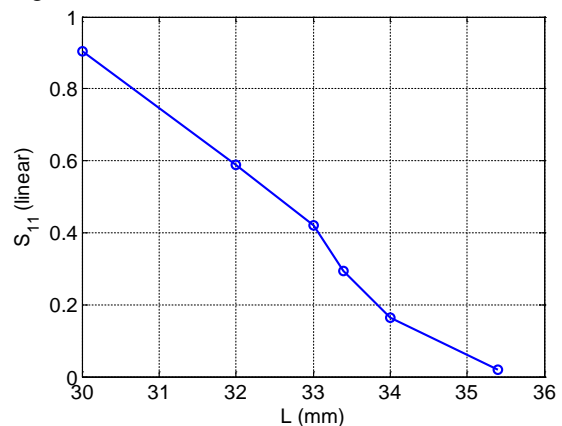


Fig. 4. Dependence of the global coefficient S_{11} on the size of input coupler hole L

As a result of coupler tuning the following values of $|R|$, $\text{Real}(R)$, $\text{Imag}(R)$, $\cos(\psi)$ were obtained at the operating frequency: 0.0068, -0.0063, 0.0025, -0.4970 respectively.

It should be noted that the values required for coupler tuning were calculated with accuracy of 10^{-3} . So these values are very sensitive to various disturbances of field structure in the system and measurement errors. On a final stage of tuning of the input coupler the measures for more precise adjustment had been taken. In particular we tried to obtain $\cos(\psi) = -0.5$ in the middle cell of the model at the linac operating frequency (Fig. 5) and to symmetrize the dependence of $\cos(\psi)$ on the longitudinal coordinate z . Nevertheless the absolute symmetrization of $\cos(\psi)$ and $|R|$ was not achieved (Fig. 6). This can indicate that field in the three regular cells of the model differ from field of homogeneous unbounded disk-loaded waveguide. From the other hand the field asymmetry in coupler cells because of coupling holes could be the reason of observed asymmetry of $\cos(\psi)$ and $|R|$. Rectangular waveguides could not be placed in the same plane due to geometrical features of the model and waveguides. Thus the asymmetry of the field in couplers influences the results of measurements.

Nevertheless the couplers were tuned. Experiments have shown that the smaller the measured value of $|R|$, the better the symmetry of the field in the model. Bandpass characteristic of the model is shown in Fig. 7.

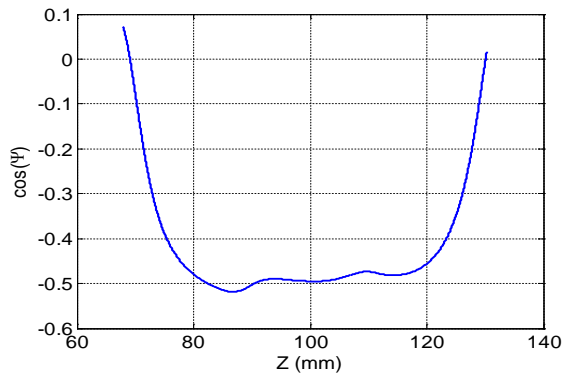


Fig. 5. Dependence of $\cos(\psi)$ on longitudinal coordinate

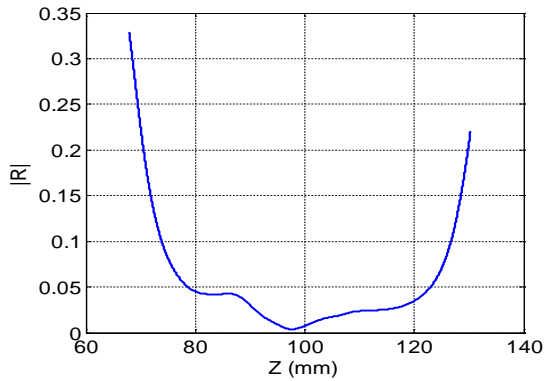


Fig. 6. Dependence of $|R|$ on longitudinal coordinate

There are five local minimums on the curve (in accordance with the number of cells in the model). Distributions of the field on the axis at the frequencies corresponding to the local minimums of S_{11} (circles in Fig. 7) are shown in Fig. 8. The midpoints of the cells are marked with vertical lines.

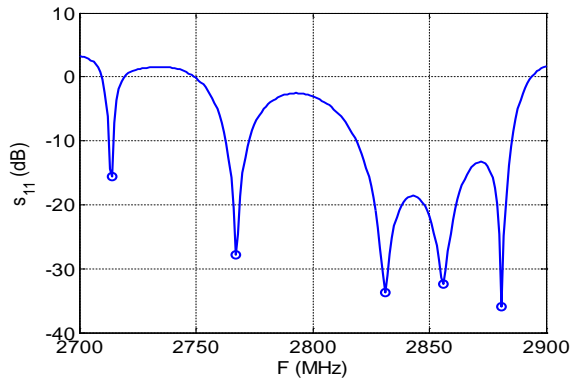


Fig. 7. S_{11} of input coupler v.s. frequency

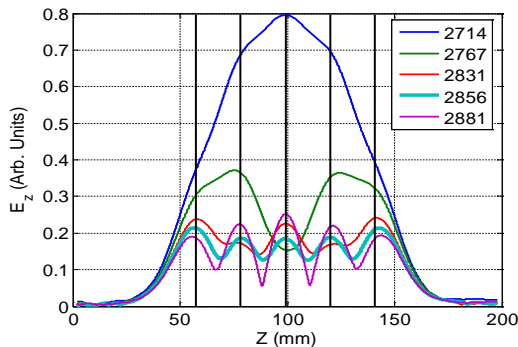


Fig. 8. Field distribution on the axis of the model for the frequencies corresponding to local minimums of S_{11} (input coupler)

The symmetrical distribution of the fields at all given frequencies (see Fig. 8) confirms the identity of the couplers in the model. Besides that at the operating frequency the reflections from the couplers are small since the appreciable change of the phase shift of the field on the period of the model ($2\pi/3$ mode) is not observed.

The analogous procedures were performed for the output coupler. The results are shown in Figs. 9-11.

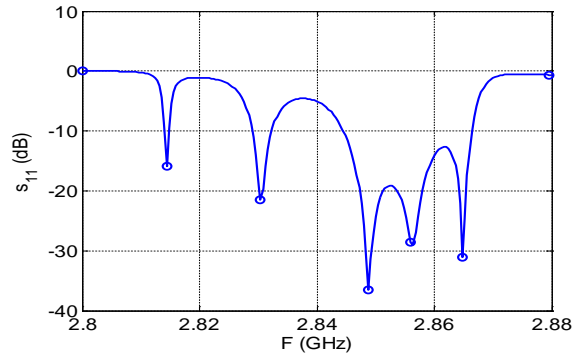


Fig. 9. S_{11} of output coupler v.s. frequency

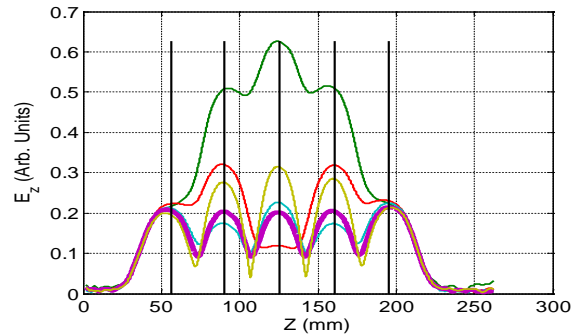


Fig. 10. Field distribution on the axis of the model for the frequencies corresponding to local minimums of S_{11} (output coupler)

Magenta curve in Fig. 10 corresponds to the operating frequency.

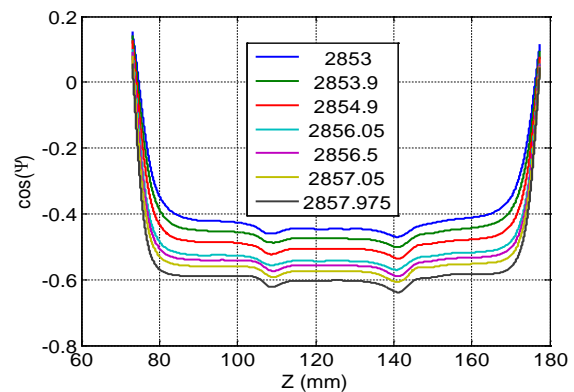


Fig. 11. Dependence of $\cos(\psi)$ on longitudinal coordinate for number of frequencies

As a result of coupler tuning the following values of $|R|$, $\text{Real}(R)$, $\text{Imag}(R)$, $\cos(\psi)$ were obtained at the operating frequency: 0.0106, -0.0079, 0.0075, -0.5319 respectively.

After tuning both couplers were braized to the section. The accelerating section was successfully tuned. The technique and results of the section tuning will be presented elsewhere.

CONCLUSIONS

The considered technique enabled us to tune the couplers for disk-loaded waveguides.

REFERENCES

1. M.I. Ayzatskiy, A.N. Dovbnaya, et al. Accelerating system for an industrial linac // *Problems of Atomic Science and Technology. Series "Nuclear Physics Investigations"*. 2012, № 4, p. 24-28.
2. W.J. Gallagher. *Measurement techniques for periodic structures*. SLAC report M-205, 1960, p. 19-31.
3. T. Khabiboulline, M. Dohlus, N. Holtkamp. *Tuning of a 50-cell constant gradient S-band travelling wave accelerating structure by using a nonresonant perturbation method*. Internal Report DESY M-95-02, 1995, p. 1-10.
4. J. Shi, A. Grudiev, A. Olyunin, W. Wuensch. Tuning of CLIC accelerating structure prototypes at CERN // *Proc. of Linear Accelerator Conf. LINAC2010*. 2010, p. 97-99.
5. N.M. Kroll, C.-K. Ng, D.C. Vier. Applications of time domain simulation to coupler design for periodic structures // *Proc. of XX Intern. Linac Conf.* 2000, p. 614-617.
6. Fang WenCheng, Tong DeChun, et al. Design and experimental study of a C-band traveling-wave accelerating structure // *Chinese Science Bulletin*. 2011, v. 56, № 1, p. 18-23
7. M.I. Ayzatskiy, E.Z. Biller. Development of inhomogeneous disk-loaded accelerating waveguides and rf-coupling // *Proc. of Linear Accelerator Conf. LINAC 96*. 1996, p. 119-121.
8. J.H. Billen, L.M. Young. POISSON/ SUPERFISH on PC compatibles // *Proc. of Particle Accelerator Conf.* 1993, p. 790-792.

Article received 02.11.2015

О МЕТОДИКЕ НАСТРОЙКИ ТРАНСФОРМАТОРОВ ТИПА ВОЛНЫ ЛИНЕЙНЫХ УСКОРИТЕЛЕЙ ЭЛЕКТРОНОВ НА БАЗЕ ДИАФРАГМИРОВАННЫХ ВОЛНОВОДОВ

Н.И. Айзацкий, Е.Ю. Крамаренко, И.В. Ходак, В.А. Кушнир, В.В. Митроченко, А.Н. Опанасенко, С.А. Пережогин, Л.И. Селиванов, В.Ф. Жигло

Приведено описание процедуры настройки входного и выходного трансформаторов типа волны (ТТВ) ускоряющей секции промышленного ускорителя электронов на базе цилиндрического диафрагмированного волновода. Показана высокая эффективность примененной методики при создании ТТВ для таких ускоряющих секций.

ПРО МЕТОДИКУ НАСТРОЮВАННЯ ТРАНСФОРМАТОРІВ ТИПУ ХВИЛІ ЛІНІЙНИХ ПРИСКОРЮВАЧІВ ЕЛЕКТРОНІВ НА БАЗІ ДІАФРАГМОВАНИХ ХВИЛЕВОДІВ

М.І. Айзацький, К.Ю. Крамаренко, І.В. Ходак, В.А. Кушнір, В.В. Митроченко, А.М. Опанасенко, С.О. Пережогін, Л.І. Селіванов, В.Ф. Жигло

Наведено опис процедури налаштування вхідного і вихідного трансформаторів типу хвилі (ТТХ) прискорювальної секції промислового прискорювача електронів на базі циліндричного діафрагмованого хвилеводу. Показано високу ефективність застосованої методики при створенні ТТХ для таких прискорювальних секцій.